The Polarized Spectrum of Anthracene.   Part III.*
The System at 3800 Å.

By D. P. Craig and P. C. Hobbins.

As briefly noted earlier (*Nature*, 1953, **171**, 566) the long-wavelength absorption system of anthracene (3750 Å in the vapour spectrum) has been studied in thin crystals at room temperature, at −140° and at about −250°, in polarized light. Frequencies and wavelengths of the absorption maxima are reported in each polarization, having been measured in several crystals at each temperature. Optical densities in the two polarizations, integrated optical densities, and the derived quantities *density ratio* and *polarization ratio* are reported to a precision limited by loss of light owing to reflection at the crystal surfaces and by the difficulty of measuring the high optical densities of the absorption maxima. Analysis of the results and comparison with the theory given in Part II * require the assignment of the absorption system to the short-axis polarized transition $A_g - B_{2u}$.

THE quantities which characterize the vapour absorption spectrum of a polyatomic molecule are the wavelengths or frequencies of the bands and the intensities of the transitions recorded in them. In only the very simplest polyatomic compounds is the rotational structure of the bands resolvable with ordinary prism spectrographs and even the bands themselves rapidly become so numerous that they merge together into broad unresolved groups. In solution these band groups, each consisting of very many bands clustered about a central frequency, are the major features of the spectrum. Usually in aromatic molecules there is one prominent progression, corresponding to the excitation of successive quanta of a single vibrational motion. In benzene the progression spacing is 920 cm.$^{-1}$, which is the frequency of the " breathing " vibration in the electronically excited state; in anthracene the spacing is about 1400 cm.$^{-1}$, presumably the frequency of one of the totally symmetrical vibrations. The vibrational structure is even more blurred in crystal spectra at room temperature, but becomes better resolved when the crystal is cooled.

In polarized light new features appear in the spectrum of the crystal characteristic of the regular arrangement of identical molecules close to one another. Naturally these new features are related to the properties of the isolated molecules and, once this relationship is theoretically understood, crystal spectra can help in assigning the molecular transitions to their symmetry species. In Part I (*loc. cit.*) the very strong absorption at 2500 Å (40,000 cm.$^{-1}$) was assigned to $A_g - B_{3u}$ from its characteristic transformation in the crystal, and in this Part we similarly analyze the weaker 3800-Å system. The cases are different in some important respects, notably that in the strong system the size of the Davydov splitting and qualitative intensity relations decide the issue, whereas here we must use subtler changes in frequency between the polarizations and rely more on measured optical densities and intensities, the significance of which has been detailed in Part II (*loc. cit.*).

The Polarization Ratio.—The two quantities characteristic of the crystal spectrum which are most valuable for interpreting the measurements to be reported in this paper are the *Davydov splitting* treated in Part I and a new quantity, the *polarization ratio*, now defined. Given the optical densities $E_a(\nu)$ and $E_b(\nu)$ for light polarized parallel to the a and b crystal axes we obtain directly the *density ratio* E_a/E_b, evaluated from the maximum values in the two polarizations. The theoretical significance of this quantity is not simple for reasons given later, and we prefer wherever possible to evaluate the ratio of the integrated optical densities over corresponding * bands or groups of bands :

$$P = \int E_a(\nu)d\nu \Big/ \int E_b(\nu)d\nu$$

The polarization ratio is the more fundamental quantity because $\int E_a(\nu)d\nu$ and $\int E_b(\nu)d\nu$ are

* Parts I and II, *J.*, 1955, 539, and preceding paper.

4 G

each proportional to the oscillator strengths of transitions in the crystal and so may be connected with the free-molecule oscillator strengths by the theory of Part II. Well-known relations between transition moment and oscillator strength being used [Part II, equation (13)], the polarization ratio is

$$\left\{ \mathscr{M}^\alpha \cdot a / |\mathscr{M}^\beta| \right\}^2 (\nu^\alpha / \nu^\beta)$$

where $\mathscr{M}^\alpha$ and ν^α are the transition moment and frequency of maximum absorption in the a component. In the practical case $\nu^\alpha \cong \nu^\beta$, and the polarization ratio is nearly enough equal to the squared ratio of transition moments. The density ratio on the other hand is useful in this fundamental way only if it is equal to the polarization ratio, *i.e.*, only if the band groups in the two polarizations have geometrically similar shapes, and this requires a similarity in the intensity distribution amongst vibrational sublevels which is not necessarily realized. In practice the density ratio shows variations from crystal to crystal and from band group to band group which, aside from all questions of theoretical significance, make it somewhat unsatisfactory as a characteristic property of the system.

Measurements at 20° *and* 60°.—Our results divide into sets according to the temperatures at which the spectra were recorded, *viz.*, 20°, 60°, —140° and the temperature of boiling hydrogen (—250°). At —250° the number of measurements was restricted by supplies of liquid hydrogen, but at the higher temperatures the spectra of some ten crystals were measured and the results averaged. Fig. 1 illustrates a typical set of results for a crystal about 0·2 μ thick at 20°. The spectrum at room temperature is poorly resolved. In each polarization there are three maxima separated to a first approximation by 1400 cm.$^{-1}$ as in solution; their relation to the vapour and solution peaks is at once apparent, with a displacement to lower frequencies by about 2000 cm.$^{-1}$ from the vapour. They will be described as forming the A progression with members $A_a{}^0$, $A_a{}^1$, $A_a{}^2$ in a polarization and $A_b{}^0$, $A_b{}^1$, and $A_b{}^2$ in b polarization. Table 1 lists wave-

TABLE 1. *Wavelengths and frequencies at* 20° *and* 60°.

	20°		60°	
	Wavelength (A)	Frequency (cm.$^{-1}$)	Wavelength (A)	Frequency (cm.$^{-1}$)
$A_a{}^0$	3922 ± 1	25,497	3920·5 ± 1	25,507
$A_b{}^0$	3931 ± 10	25,439	3933 ± 9	25,426
$A_a{}^1$	3716 ± 1·4	26,911	3714 ± 1	26,925
$A_b{}^1$	3725 ± 4	26,846	3722 ± 1·5	26,867
$A_a{}^2$	3524 ± 0·7	28,377	—	—
$A_b{}^2$	3529 ± 1·7	28,337	3523 ± 1·5	28,385

* The idea of corresponding bands has force only in terms of the weak-coupling model treated in Parts I and II, where one thinks of a band in a polarization and another in b as a pair derived by perturbing one free-molecule band.

lengths and frequencies for these maxima at 20° and 60°. The errors are standard deviations, based usually on five or six measurements at 20° and four at 60°. Measurements of the b maxima show considerable scatter and are not precise enough except in one or two cases in Table 1 for calculating the Davydov splitting and other frequency differences. There is a barely significant temperature displacement of wavelengths between 60° and 20°; we believe it to be real, since a further displacement in the same sense occurs between 20° and —140°. The difference between the frequency of the n-th maximum in one polarization and the corresponding maximum in the other is measured by $A_a{}^n - A_b{}^n$: we continue to describe this interval as the Davydov splitting, although as shown in Part II it arises only partly from the effect which Davydov considered and partly from second-order effects. We are concerned also with the intervals to be referred to as *progression intervals* between successive maxima in a given polarization, measured by differences of the type $A_a{}^1 - A_a{}^0$. These intervals in vapour and solution are constant, but are disturbed rather irregularly in the crystal. Values of some derived quantities are listed in Table 2, based on the more precise results in Table 1.

The increased progression interval between the second and third members is significant

and is confirmed by measurements at lower temperatures. Its importance is discussed below.

The optical densities of the crystals in the two polarizations were measured as described in Part I and the density ratios found. These ratios are unsuitable for averaging because

TABLE 2. *Splittings and progression intervals at room temperature.*

Davydov splitting		Progression intervals (solution value 1412 cm.$^{-1}$)			
$A_a^1 - A_b^1$	65 ± 31 cm.$^{-1}$	$A_a^1 - A_a^0$	1414 ± 12 cm.$^{-1}$	$A_b^1 - A_b^1$	1491 ± 32 cm.$^{-1}$
$A_a^1 - A_b^1$	58 ± 13	$A_a^1 - A_a^0$	1418 ± 10	$A_b^2 - A_b^1$	1518 ± 16
$A_a^2 - A_b^2$	40 ± 5	$A_a^2 - A_a^1$	1466 ± 12		

of the varying reflection loss from the crystal surfaces. This may be equivalent to an optical density in the range 0—0·10 or even 0·15 added to the desired optical density due to absorption. The crystals used are less than a wavelength thick and interference effects

FIG. 1. *Polarized spectrum of anthracene at 20°.*
Upper curve : absorption parallel to *b* crystal axis.
Lower curve : absorption parallel to *a* crystal axis.
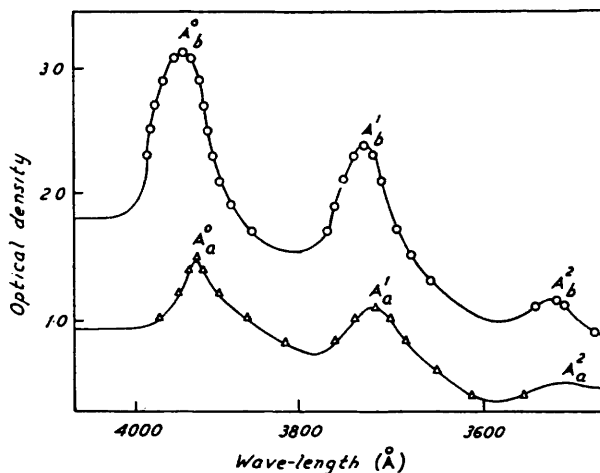
complicate the reflection behaviour * ; under these conditions the dependence of loss on crystal thickness and on wavelength is bound to be sensitive. Reflection is relatively less important compared to molecular absorption for thick crystals than for thin; but thick crystals have high optical densities intrinsically more difficult to measure accurately. The results for several crystals are set out in Table 3. No correction to these values has been made for the reflection loss.

These values are very scattered. A nearly constant set of results is found by measuring the polarization ratio, recorded in Table 4 for three different crystals for which results were available complete enough to carry out the required integrations of optical density.

TABLE 3. *Density ratios (E_a/E_b) at absorption maxima (20° and 60°).*

A^0	A^1	A^2	A^0	A^1	A^2
—	—	1/1·8	1/1·9 *	1/1·8	1/1·5
1/2·4	—	—	1/1·9 *	1/1·7	—
—	—	1/1·7	1/1·7 *	1/1·8	1/1·8
1/2·1	1/2·7	—	1/2·3 *	1/1·8	1/1·4
1/1·6	1/1·7	1/1·4		* At 60°	

TABLE 4. *Polarization ratios at 60°.*

A^0	A^1	A^2	Overall
1/2·0	1/1·7	1/1·4	1/1·7
1/2·0	1/1·8	1/1·7	1/1·8
1/2·1	1/1·6	1/1·4	1/1·7

Values of the polarization ratio have not previously been recorded, and the only result which is at all comparable relates to a measurement of the fluorescence emission of crystalline anthracene by Ganguly and Choudhuri (*J. Chem. Phys.*, 1951, **19**, 617). There

* Dr. L. E. Lyons kindly drew our attention to cases in which the transmission of a silica disc plus thin crystal is greater than that of the disc alone, suggesting a negative reflection loss by the principle of the coated lens.

is a well-known mirror symmetry between absorption and fluorescence in vapour and solution spectra and reference to the theory of Part II shows that this principle has an application also in crystals. Fluorescence is predominantly from the lowest excited state and one should find that the emitted light is polarized in the same ratio as the light absorbed in the first member of the absorption progression. The overall polarization ratio in fluorescence should therefore be near to, but slightly greater than, the overall ratio in absorption. Ganguly and Choudhuri analyzed the fluorescence emission with an optical system with which they could find the direction of maximum intensity in relation to the crystal axes. They found that this direction made an angle of 33° with the b crystal axis, a result which may be interpreted to mean that the b polarized emission is $\cot^2 33° = 2\cdot4$ times stronger than the a emission. This is greater than the overall absorption ratio (1·8) and even somewhat greater than the ratio for A^0 (2·0). The agreement must however be treated with caution, since a fraction of the excited molecules lose their energy otherwise than by fluorescence. Little is known of the details of this degradation which, if it drained off one excited state polarization more than the other, could upset the emission polarization ratio from the theoretical value.

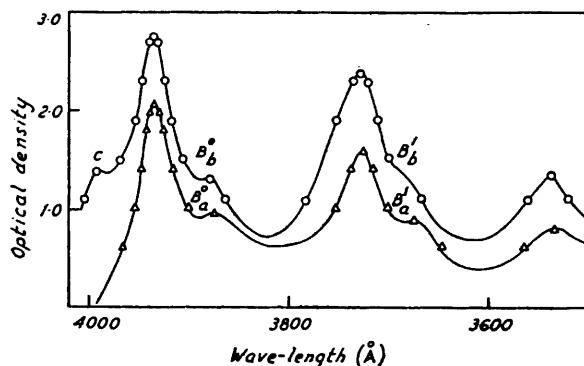*Measurements at* −140°.—A typical spectrum at −140° is illustrated in Fig. 2. Com-

FIG. 2. *Polarized spectrum at* −140°.

Upper curve : parallel to b crystal axis.
Lower curve : parallel to a axis.

The three main maxima are the A series, as in Fig. 1.

pared with room-temperature spectra its maxima are better resolved and additional structure has appeared. B^0 and B^1 appear in both polarizations and clearly form the beginning of a progression distinct from the A series; band C shows only in b absorption, and no corresponding a absorption was found in any of the crystals examined at this temperature. Table 5 lists the wavelengths averaged over results for eight crystals.

TABLE 5. *Wavelengths and derived quantities at* −140°.

Wave-length (Å)		Frequency (cm.⁻¹)	Derived quantities	
			Davydov splitting (cm.⁻¹)	
A_a^0	3931·5 ± 1·3	25,436		
A_b^0	3934 ± 1	25,419	$A_a^0 − A_b^0$	17 ± 11
B_a^0	3874·5 ± 1	25,810	$A_a^1 − A_b^1$	29 ± 10
B_b^0	3880 ± 1	25,773	$A_a^2 − A_b^2$	48 ± 15
A_a^1	3725 ± 1·2	26,846		
A_b^1	3729 ± 0·7	26,817	Progression intervals (cm.⁻¹)	
B_a^1	3674 ± 0·7	27,218	$A_a^1 − A_a^0$	1410 ± 12
A_a^2	3532 ± 1	28,313	$A_b^1 − A_b^0$	1398 ± 9
A_b^2	3538 ± 1·5	28,265	$A_a^2 − A_a^1$	1467 ± 12
C_b	3989·5 ± 1·7	25,066	$A_b^2 − A_b^1$	1448 ± 13
			$B_a^1 − B_a^0$	1408 ± 9

The optical densities of all eight crystals were measured and values of the density ratio derived. Averaged values for the three members of the A progression, reflection losses being disregarded, are : A^0 1/1·4, A^1 1/1·6, A^2 1/1·7, and B^0 1/1·7. The density ratios show a very considerable scatter, but as at room temperature (Table 4) the overall polarization ratios are markedly constant in the range 1·7—1·8. Moreover in one crystal studied both at room temperature and at −140° the polarization ratio showed no change with temperature.

Measurements at about 20° K.—A limited number of spectra were recorded at the temperature of boiling liquid hydrogen in a specially constructed cell described below. The most complete single set of results is shown in Fig. 3. Structure at the long wavelength onset of absorption was partly obscured by heavy plate blackening in the spectrum illustrated in Fig. 3; in a thicker crystal more structure was visible. This is shown in Fig. 4, and the new bands are recorded in Table 6. Two crystals only could be studied at this temperature and the accuracy of the measurements is difficult to assess. Where a standard deviation is shown several measurements have been made and averaged, otherwise only one or two. The maxima were, however, in general much sharper than at −140° and an individual measurement correspondingly easier to make precisely.

The shift to longer wavelengths with decreasing temperature is confirmed by these values. The Davydov splittings and progression intervals derived from Table 6 agree within
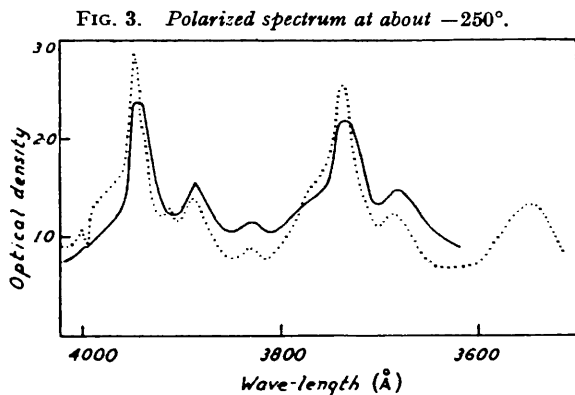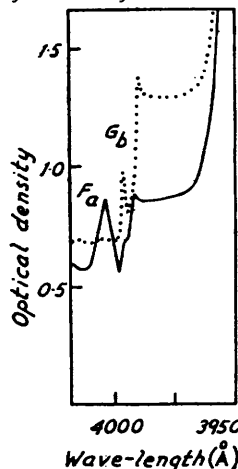

FIG. 3. *Polarized spectrum at about* −250°.

FIG. 4. *Long-wavelength onset of absorption at about* −250° *obtained with a slightly thicker crystal than* FIG. 3.

reasonable limits with values obtained at −140°. The main importance of these measurements however, to be discussed on p. 2315, is in showing variations of the density ratio in different regions of the spectrum. In the ranges where absorption is weak, absorption in *a* polarization is greater than in *b*, but where absorption is strong the *b* component is

TABLE 6. *Measurements at* −250°.

	Wavelength (Å)	Frequency (cm.⁻¹)		Wavelength (Å)	Frequency (cm.⁻¹)
F_a	4002	24,988	D_a^0	3828	26,123
G_b	3995 ± 1	25,031	D_b^0	3830	26,110
C_a	3991	25,056	A_a^1	3733 *	26,788
C_b	3989 ± 1·5	25,069	A_b^1	3738 *	26,752
A_a^0	3945 *	25,349	B_a^1	3680 *	27,174
A_b^0	3945 ± 2	25,349	B_b^1	3686 ± 0·8	27,130
B_a^0	3884 ± 0·8	25,747	A_b^2	3546	28,201
B_b^0	3887 ± 1	25,727			

* Single measurement only.

stronger than *a* (Fig. 3). At higher temperatures *b* absorption exceeds *a* throughout the system.

We are able to compare our results at this temperature with those of Obreimov and Prikhotjko (*Phys. Z. Sowjetunion*, 1936, **9**, 34) who were the first to record a low-temperature crystal spectrum in polarized light. Their work established the general character of the crystal spectrum and showed *b* absorption to be greater than *a*. For reasons connected with the low dispersion of the spectrograph, their wavelength measurements were not exact enough to prove a Davydov shift nor to establish perturbations in the vibrational

intervals, and there are some minor features of their results, such as a splitting in the intense *a* maximum, which our plates do not show. More important is their conclusion that there are several very sharp bands in the *b* spectrum which are missing in the *a*, namely at 4037, 4005, 3991, 3981, 3916, 3857, 3848, and 3805 Å. The strongest of these is at 3991 Å, band *C* in Table 6. There is no doubt that this occurs in both polarizations as shown in Fig. 4; its *a* component however was only detected at low temperatures and in a rather thick crystal, otherwise it tends to be hidden by $A_a{}^0$. Not all of the other bands were visible under the conditions used for our plates, but those which do appear, such as F_a at 4002 Å, seem to do so always in both polarizations even though as in this case the weaker component is ill-defined. Clearly, more work at very low temperatures will be needed to study these sharp and weak bands, but our work goes to show that they have components in both polarizations and do not therefore call for a novel explanation. Table 7 compares some wavelength values from Obreimov and Prikhotjko (*loc. cit.*) with ours.

TABLE 7. *Wavelengths* (Å).

Band group	$A_a{}^0$	$A_b{}^0$	$A_a{}^1$	$A_b{}^1$	$A_b{}^2$	$B_a{}^0$	$B_b{}^0$
Obreimov and Prikhotjko ...	3940	3938	3719	3735	3548	3885	3887
Present work	3945	3945	3733	3738	3546	3884	3887

Interpretation of the Measured Davydov Splittings and Progression Intervals.—The allowed transitions in anthracene belong either to the species $A_g - B_{2u}$ (short axis polarized) or $A_g - B_{3u}$ (long axis polarized). If the transition is electronically allowed the species symbols refer to electronic symmetry properties; if not they refer to vibronic (electronic $\times$ vibrational) symmetry and our discussion applies equally to both. It is convenient to leave a decision between them until the overall symmetry has been settled. The intense system at 2500 Å belongs to the long axis species $A_g - B_{3u}$ (Part I) and is electronically allowed. In proceeding to assign the band system at 3800 Å to its symmetry species we shall consider separately the two results typical of the crystalline state, namely, the Davydov splittings and progression intervals on the one hand and the polarization ratio on the other. It is beyond doubt that, where the splitting occurs, it involves a *b* component displaced to lower frequencies and an *a* component to higher. The results at $-140°$ determine the splitting most accurately (Table 5). It is in the range 10—50 cm.$^{-1}$, and is less for the zero-quantum state than for the others. Table 8 compares the values at $-140°$

TABLE 8. *Calculated and found values of splittings and progression intervals at* $-140°$.

	Davydov splitting (cm.$^{-1}$)				Progression intervals (cm.$^{-1}$)		
	Found	Calc. for $A_g - B_{3u}$	Calc. for $A_g - B_{2u}$		Found	Calc. * $A_g - B_{3u}$	Calc.* $A_g - B_{2u}$
A^0	17	217	29	$A_a{}^1 - A_a{}^0$	1410	1483	1427
A^1	29	282	31	$A_b{}^1 - A_b{}^0$	1398	1418	1425
A^2	48	225	25	$A_a{}^2 - A_a{}^1$	1467	1397	1465

* By taking the vapour splitting as 1412 cm.$^{-1}$.

with values calculated in Table 2 of Part II for the two allowed assignments in anthracene. The splittings are incompatible by an order of magnitude with the long axis assignment $A_g - B_{3u}$ but they agree as well as can be expected with the short axis $A_g - B_{2u}$. The progression intervals, also in Table 8, give a less definite indication; the best established experimental fact is that the interval $A^2 - A^1$ is greater than $A^1 - A^0$ by a substantial margin outside the experimental error. This feature appears in calculations for $A_g - B_{2u}$ and not for $A_g - B_{3u}$ and so the former assignment is supported; the numerical agreement is not, however, uniformly good.

Interpretation of the Measured Polarization Ratio.—The theoretical value of the polarization ratio in a weak system has been discussed in Part II (*loc. cit.*). For the oriented gas model a long and a short axis system are associated respectively with ratios 16 : 1 and 1 : 7·8. According to Part II a weak system would not give values at all close to these. For a system like that of anthracene at 3800 Å, due allowance being made for a strong long axis system nearby, the calculated values are near 2·3 : 1 and 1 : 3·0. These figures apply to a weak system which in the free molecule is entirely of one polarization. However, aside

from crystal perturbing forces it is possible that intramolecular vibrations may also transfer intensity from strong transitions to weaker ones. The only well-understood example of vibrational perturbations in a complex molecule is that of benzene where the whole of the intensity in the 2600 Å system ($f = 0\cdot002$) and in the 2000 Å system ($f = 0\cdot1$) is vibrationally induced. Herzberg and Teller's theory of the effect (*Z. phys. Chem.*, 1933, **21**, *B*, 410) shows the borrowed intensity to be proportional to the first power of the intensity of the perturbed strong system and to the inverse square of its energy separation from the weak one. Assuming other factors to be equal, and noting that the intense system in anthracene is twice as strong as in benzene, we find that the stolen intensity in the 3800 Å anthracene system is between $f = 0\cdot005$ and $0\cdot05$. Its polarization, like that of the strong system, must be parallel to the long axis, and from the crystal structure the stolen intensity amounts to between $f = 0\cdot0037$ and $0\cdot037$ along the *a* axis and one sixteenth as much along *b*. These are probably minimum values because in bigger molecules the vibrational amplitudes are usually greater, so that one expects an increased effect in anthracene; but a value within these limits will account for the observed results. Vibrationally borrowed intensity would not coincide with the maximum of the allowed component; the system might behave as do substituted benzenes in the 2600 Å system, namely, have a forbidden progression displaced from the allowed progression by the frequency of a non-totally symmetrical vibration, and, provided the forbidden intensity were great enough, it should be detectable in the troughs between the allowed maxima, especially as its polarization is opposite, with $E_a > E_b$. In spectra at liquid-hydrogen temperature (see p. 2313) such regions were found which suggested that the system was a mixture of allowed and forbidden components. The resolution of the *a* polarized zones is poor and since they are of secondary importance to the assignment of the main system they were not studied further. Compared to the wavelength measurements, which are fairly straightforward, measurements of crystal optical densities are subject to at least two errors, particularly when considerations of crystal thickness demand the measurement of inconveniently high optical densities. The errors introduced by reflection have been discussed (p. 2311). We have no satisfactory measure of the reflection loss but, by analogy with the properties of light in transparent media, take it to correspond, at most, to an effective optical density of $0\cdot1$—$0\cdot15$ unit. The contribution of reflection to the measured intensites $\int E_a \mathrm{d}\nu$ and $\int E_b \mathrm{d}\nu$ may be assessed and subtracted; the range of integration is about 3600 cm.$^{-1}$ and the reflection " intensity " is therefore about 360, or 540 in the extreme case. In a typical measurement the measured ratio is $8500/4700 = 1\cdot8$; the maximally corrected value falls near $1\cdot9$. Evidently the correction is small even under extreme conditions.

The second error arises when, in measuring high values of the optical density, we compare the plate blackening by light which has passed through the crystal with that in which a high optical density has been simulated by a rotating sector and a reduced time of exposure. Failure of the photographic reciprocity law may then give incorrect results (see p. 2318 for a detailed discussion). Essentially, high values tend to be measured as too high, making the density ratio and, to a lesser extent, the polarization ratio, high also. This effect was minimized by using the reduced exposure method only where absolutely necessary, *i.e.*, in the highest optical densities. Thus the wavelength range over which the error can occur, and the error in the integrated optical density, are small; it could not exceed $0\cdot1$ in the polarization ratio, reducing the measured $1\cdot8$ to $1\cdot7$. On the other hand the density ratio is very sensitive to the values at the maxima and this probably explains its erratic behaviour.

We now consider actual values. The calculated values in Table 2 of Part II show that the system must be assigned to $A_g - B_{2u}$ and not $A_g - B_{3u}$. The latter requires a polarization behaviour in which the *a* component is the stronger, which conflicts with experiment, whereas the former makes the *b* component stronger, as is actually found. The experimental ratios, with those calculated given in parentheses, are $1/2$ ($1/3$), $1/1\cdot7$ ($1/2\cdot8$), $1/1\cdot5$ ($1/2\cdot6$). The discrepancy arises mainly from the mixture with the main system of a vibrationally induced long axis component and not from the small reflection and reciprocity

errors, which oppose one another. We consider that the vibrationally induced intensity is about 20% of the whole. This leads to a reasonably satisfactory agreement, but neither the theoretical nor the experimental accuracy justifies elaborate computations. We now consider whether the system $A_g - B_{2u}$ is electronically allowed or, like the long axis component, allowed only through vibrational perturbation of some other system. There is no direct evidence from our measurements but two arguments are against assignment to an electronically forbidden transition. First, it is improbable on grounds of magnitude. The nearest intense short axis system begins near 2000 Å, separated by 25,000 cm.$^{-1}$ from the weak system. By analogy with benzene, intensity borrowing here would not exceed $f = 0.02$, only one fifth of the observed value. Secondly, experience suggests that a forbidden system would reveal itself in solution, as in benzene, with a weak but definite 0—0 band to long wavelengths of the main system. The careful study of the solution spectrum over a range of temperature and down to very low values of extinction coefficient made by Broderson and Langseth (*Dansk Mat. Fys. Medd.*, 1951, **3**, 26) would have shown such structure if it existed, but none was found. The assignment is therefore to the allowed *electronic* species $A_g - B_{2u}$.

A further confirmation is in the comparison of the total intensity of the weak system in the crystal with that in solution. The necessary geometrical relations between solution and crystal values were given in Part I. A short axis system, before allowance for interaction with other systems, should have an optical density per micron of $2.17 \times 10^{-4}E_s$ parallel to the a axis and $1.69 \times 10^{-3}E_s$ parallel to b, E_s being the solution extinction coefficient of about 10^4 units. The transfer effect makes little difference to the b component, which is better for this comparison. Our crystals were 0.1—0.2 micron thick, and the b optical density should have fallen in the range 1.7—3.4 : its value was usually near 3.0, in good agreement with expectation and in further support of the short axis assignment.

Short axis polarization has been widely credited to this system in anthracene, mainly because of the molecular-orbital prediction discussed below. Most previous experimental work has been done with unpolarized light and so is not relevant. Obreimov and Prikhotjko (*loc. cit.*) and Ganguly and Choudhuri (*loc. cit.*) showed respectively that absorption and fluorescence are stronger along the b than the a axis, but these results could not be interpreted until the assignment of the intense system at 2500 Å was established. Aside from our earlier report (*Nature*, 1953, **171**, 566) the only relevant work is the spectrum of anthracene in durene (McClure, *J. Chem. Phys.*, 1954, **22**, 1256). Making reasonable assumptions about the orientation of the embedded molecules McClure found absorption to be concentrated along the short axis and assigned the system $A_g - B_{2u}$, in agreement with us. Jones (*Chem. Rev.*, 1947, **41**, 353), without using polarized light, but by studying the spectral effects of substitution in different positions in anthracene, came to the same conclusion.

Comparison with Theory.—Energy levels of anthracene have been calculated by at least three distinct forms of π-electron theory. Forster (*Z. phys. Chem.*, 1938, **41**, B, 287) used the valence-bond method and predicted that the lowest singlet excited state would be of species B_{3u}, a conclusion which we have shown to be incorrect. Coulson (*Proc. Phys. Soc.*, 1948, **60**, 157) and Platt (*J. Chem. Phys.*, 1950, **18**, 1168), using molecular-orbital theory in its LCAO and free-electron forms, respectively, predicted correctly that the first excited state would be B_{2u} and the second B_{3u}. Moffitt (*J. Chem. Phys.*, 1954, **22**, 320) has recently developed Platt's scheme and made possible quantitative calculations of transition energies and oscillator strengths. Having now two experimentally established assignments in anthracene, we may compare the true oscillator strengths with values calculated in the LCAO–MO theory and in Moffitt's *perimeter model* (Table 9).

TABLE 9. *Calculated and found oscillator strengths in anthracene.*

	Experimental	LCAO–MO	Perimeter model
Lowest singlet	$A_g - B_{2u}$: f . . . 0.1	0.9	0.37
Second singlet	$A_g - B_{3u}$: f . . . 2.3	1.4	4.8

LCAO–MO theory appears to be equally suitable for the higher linear polycyclic hydrocarbons tetracene and pentacene, but not for naphthalene. According to theory, naphthalene should show the same sequence of ultraviolet-band systems as anthracene,

with somewhat higher transition energies; but the spectrum shows an additional very weak band system at 3200 Å which cannot be fitted into the LCAO–MO scheme. This weak system is found in free-electron calculations, in those based on the perimeter model, and in the non-empirical configurational interaction approximation (Jacobs, *Proc. Phys. Soc.*, 1949, **62**, 710) : the predicted assignment is $A_g - B_{3u}$. This is one of two assignments which are compatible with experimental evidence, the earlier part of which has been reviewed by one of us (Craig, *Rev. Pure Appl. Chem.*, 1954, **3**, 207).

EXPERIMENTAL

The Crystals.—Anthracene (B.D.H. " blue fluorescing ") was purified by chromatography on alumina in light petroleum (b. p. 40—60°) in darkness to avoid photo-oxidation of adsorbed anthracene to anthraquinone, which occurs rapidly in daylight. The pure anthracene was eluted and crystallized (m. p. 218°). It did not phosphoresce with ultraviolet light when dissolved in a rigid glass of ether–2-methylbutane–alcohol.

Thin crystals were produced by rapid sublimation in an inert atmosphere. A small cylindrical furnace made from 1″ copper tube 1·5″ long and wound with a 50-ohm heating coil encased in fireclay was placed on a hot-plate. A Pyrex beaker fitted the furnace; the hot-plate was heated initially to 100° and the beaker filled with solid carbon dioxide or with nitrogen gas. A small amount of anthracene was put in and the heater closed by a filter paper held down by a crucible lid. The hot-plate was then switched off and the heater run at 1·5 A for 1—2 min. Sublimation continued for 5—10 min.; crystals formed inside the porcelain lid and on the filter paper. The former were usually thinner, varying with the conditions; the thinnest showed blue or golden interference colours and were 0·1—0·2 µ thick. Measurements were usually made with the crystals mounted on a polished silica disc to which they were transferred on an electrically charged needle from the sublimation surface.

Obreimov and Prikhotjko (*loc. cit.*) reported that sublimation leaflets of anthracene crystallize regularly and in the (001) orientation. This was of central importance to our work, and at our request Dr. Philip Knight of the Department of Crystallography, University College, made a number of X-ray examinations of crystals of different thicknesses and from different batches to confirm it. The orientation was always found to be (001). The well-developed crystal face thus contains the *a* and *b* monoclinic axes, and it was found by microscopy that the *b* axis corresponded to the slow vibration direction. This fact allowed all other crystals to be aligned with their *a* and *b* axes along the electric vector vibration directions by microscopy alone.

We had no very satisfactory way of measuring crystal thickness but used the two following approximate methods. (i) From Newton's colour scale retardations were found by identifying interference colours. The thickness *d* is then given by the formula $R = d(\beta - \alpha)$, where the bracketed quantity is the birefringence in the *ab* plane, *R* is the thickness, and *d* the retardation. For anthracene, $R = d(1·79 - 1·63)$. (ii) The surface area of a thin crystal was estimated as closely as possible. The crystal was dissolved in a known volume of alcohol and the optical density of the solution measured with a Cary recording spectrophotometer in the region of intense absorption near 2500 Å. The concentration of the solution being thus determined, the thickness of the crystal was calculable. The agreement with (i) was within a factor of 2 and is the basis for the earlier statements here and in Part I that the thickness of the best crystals was about 0·1—0·2 µ.

Spectroscopic Methods.—Two spectrographs, Hilger types E1 and E492, both large quartz Littrow instruments with the same optics, were used. The plates used were : 4500—3000 Å, Ilford Special Rapid; 3000—2500 Å, Ilford Q1; 2500—2000 Å, Ilford Q2.

For work below 3500 Å a small 500 mA hot cathode hydrogen discharge lamp was used as the light source, running at constant voltage. Above 3500 Å the stray line spectra from the hydrogen lamp were disturbing and the best source was a Siemens P28/25 strip lamp running at 6 v, 18 A. The lamp was mounted with the tungsten strip in a horizontal plane to minimize temperature variations. Light from the strip was reflected into the optical system from an aluminium mirror at 45°. In experiments with a rotating sector it was necessary to run the lamp from accumulators to eliminate beat effects between the periods of the sector and brightness fluctuations.

Light from the source was focused on to the crystal in its holder by a fused silica lens (Fig. 5). The transmitted light entered the Wollaston unit and came to a pair of foci at the slit, each plane polarized, and with the planes perpendicular to one another. The separation of the beams was

4 mm. The Wollaston unit held the prism itself (2 cm. aperture) and two plano-convex fused silica lenses of focal length 20 cm. at 3200 Å facing opposite sides of the prism and adjustable so that parallel light entered the prism at any chosen wavelength. Careful alignment was necessary to ensure that both beams in a blank exposure have the same intensity. This condition was satisfied when both beams illuminated the same area of the spectrograph prism symmetrically about its centre line.

Microphotometer records were taken of all plates by use of a Zeiss microphotometer. Iron-arc spectra were photographed on the plate between the two polarized crystal absorptions and each microphotometer record was run twice, once to draw the trace of the absorption and a second time to draw the iron arc spectrum. The record was then read with a travelling microscope, wavelengths being measured by linear interpolation between closely spaced iron lines. The method for measuring optical densities has been briefly described in Part I. A series of blank exposures was made with the same exposure time as for the absorption spectrum of the crystal. Successive exposures were reduced in intensity by a rotating sector, giving a set of plate blackenings corresponding to known optical densities. The spectrum of the crystal was then recorded on the microphotometer on the same record as an optical density blank. The traces crossed at " match points." From a set of such records values of optical density were assembled as a function of wavelength. The error introduced by a second more convenient method was found to be negligible : this was to superimpose a trace of the absorption spectrum upon traces of known, sectored, optical density taken from a second plate developed under identical conditions, and then to measure the wavelengths of the match points.

FIG. 5. *External optical system showing the source at the left-hand end, then a fused silica lens, the crystal holder, the Wollaston prism unit, and the spectrograph slit at the right. $X + Y + Z = 24 \cdot 2$ cm. The Wollaston unit as a whole was kept fixed, but the two lenses in it were movable, to allow the light through the prism to be made parallel at any wavelength.*
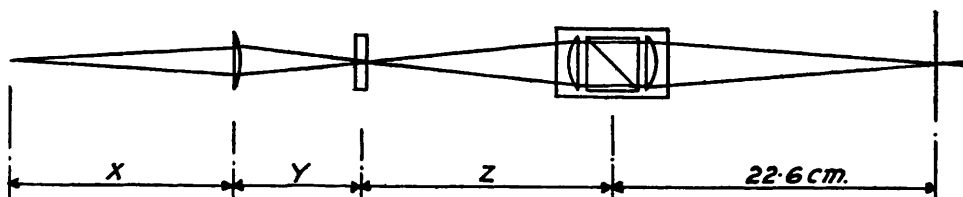
Our programme of measuring optical densities of the same crystal in two polarizations made it inevitable to work at higher optical densities than available with a rotating sector. The two polarizations differ in intensity by a factor of about 2, so that even if one can be measured at the optimum density, say 0·8, the other is unfavourably high or low. The method used for high optical densities involved as an extra feature a fixed sector setting and logarithmically decreasing exposure times, beginning with the same exposure as used for the crystal spectrum (15 min.). An undesirable aspect is the possible failure of the photographic reciprocity law but by using the variable exposure method only for the highest optical densities, and by repeating all measurements of density and polarization ratio on several crystals of different thickness we could ensure that the errors were small. The optical densities measured by varying the exposure tend to be high : the photographic efficiency for short exposures of the emulsions used is greater than for the 15 min. crystal exposures, giving greater plate blackenings in the comparison runs than for strict proportionality. Match points are obtained with spuriously short comparison exposures, and therefore at too high optical densities. Published curves suggest a maximum error of 0·3 density units under our conditions. This error, if it occurred, would be directly shown in the density ratios which tend to be too high ; but its effect is rather small in the polarization ratio, since the integrated intensities are affected only by a small part of the range of integration, and for the greater part the density values involve no reciprocity error at all (sector method) or a negligible one (exposure ratio 5 : 1 or less).

Low-temperature Cells.—A very simple cell (Fig. 6) was found adequate for temperatures in the range 60° to −140°. One face of a hollow brass cube of side 8 cm. was removed and replaced by a hollow pyramid, with a 2·5 cm. square opening at the top. Two round holes were drilled in opposite faces of the cube and a brass tube (3·5 cm. dia.) inserted. Two similar tubes, each having one end closed by a silica window, could be screwed into the end of this tube, making a closed cylinder of which the centre part was surrounded by the brass cube, and so cooled or heated by its contents. The centre section contained an annular stop against which the crystal

on its mount could be held. Even when liquid air was used as refrigerant no condensation took place on the crystal, but it was necessary to stop condensation on the end windows with jets of air. The temperature measured at the position of the crystal was $-140°$ with liquid air as cooling agent.

For work with liquid hydrogen the more elaborate cell shown in Fig. 7 was constructed. In this case the central section of the tube holding the crystal joins the rest of the cell only

FIG. 7. *Cell for use with liquid hydrogen as refrigerant. Brass is used throughout except for the thin tube of German silver joining the inner reservoir and sample tube to the rest of the apparatus. The hydrogen reservoir is surrounded by an evacuated space, and the outermost container holds an alcohol–CO_2 cooling mixture.*

FIG. 6. *Cell for temperatures down to $-140°$.*
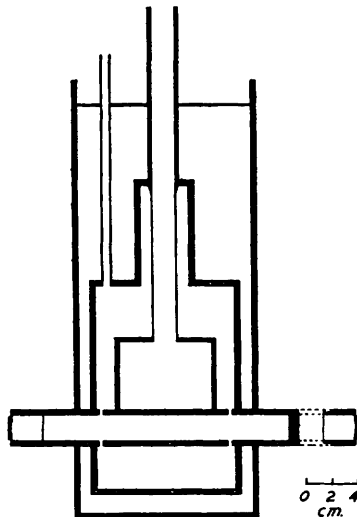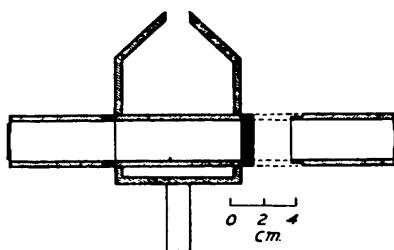
through the poorly conducting thin (0·1—0·2 mm.) German-silver tube to the exterior of the Dewar flask. The end pieces to which the quartz windows were fixed with Araldite cement screwed in as shown and were greased with Silicone grease as lubricant and vacuum seal. The windows were heated to keep them free from ice. At the beginning of a run the outer jacket was filled with dry ice. After 30 min. liquid oxygen was put into the reservoir and after another 30 min. the Dewar flask was slowly evacuated through a capillary, the crystal being by this time cold enough to resist damage and distortion. After another 30 min., when the last drop of oxygen had evaporated, liquid hydrogen was siphoned in and, after conditions became steady, the run was started. The crystal was probably cooled to *ca.* 20·4° k, the b. p. of hydrogen.

WILLIAM RAMSAY AND RALPH FORSTER LABORATORIES,
    UNIVERSITY COLLEGE, LONDON.
DEPARTMENT OF PHYSICAL CHEMISTRY,
    UNIVERSITY OF SYDNEY. [*Received, January 11th,* 1955.]